THE UNIVERSITY OF ALABAMA® | University Libraries

Fluid/Kinetic Hybrid Simulation of Atmospheric Escape: Pluto

Orenthal J. Tucker – University of Virginia
Justin T. Erwin – University of Virginia
Robert E. Johnson – University of Virginia
Alexey N. Volkov – University of Virginia
Timothy A. Cassidy – Jet Propulsion Laboratory

Deposited 10/12/2018

Citation of published version:

Tucker, O., Erwin, J., Johnson, R., Volkov, A., Cassidy, T. (2011): Fluid/Kinetic Hybrid Simulation of Atmospheric Escape: Pluto. *AIP Conference Proceedings*, 1333(1). DOI: 10.1063/1.3562798

© 2011 American Institute of Physics.

Fluid/Kinetic Hybrid Simulation of Atmospheric Escape: Pluto

Orenthal J. Tucker, Justin T. Erwin, Robert E. Johnson, Alexey N. Volkov, and Timothy A. Cassidy

Citation: AIP Conference Proceedings **1333**, 1145 (2011); doi: 10.1063/1.3562798
View online: https://doi.org/10.1063/1.3562798
View Table of Contents: http://aip.scitation.org/toc/apc/1333/1
Published by the American Institute of Physics

Fluid/Kinetic Hybrid Simulation of Atmospheric Escape: Pluto

Orenthal J. Tucker[a], Justin T. Erwin[a], Robert E. Johnson[a], Alexey N. Volkov[a] and Timothy A. Cassidy[b]

[a]*Department of Materials Science and Engineering, University of Virginia, Charlottesville, VA 22904, USA*
[b]*Jet Propulsion Laboratory, Pasadena, CA*

Abstract. A hybrid fluid/molecular kinetic model was developed to describe the escape of molecules from the gravitational well of a planet's atmosphere. This model was applied to a one dimensional, radial description of molecular escape from the atmosphere of Pluto and compared to purely fluid dynamic simulations of escape for two solar heating cases. The hybrid simulations show that the atmospheric temperature vs. altitude and the escape rates can differ significantly from those obtained using only a fluid description of the atmosphere.

Keywords: Jeans escape, Slow Hydrodynamic, Pluto, Thermal escape.
PACS: 92.60.H

I. INTRODUCTION

Pluto's slow rotational period and highly eccentric and oblique orbit results in significant changes in its atmospheric density. For example, since 1989 the dwarf planet has been receding from perihelion and, surprisingly, observations suggest that its atmospheric volume has doubled [1]. Pluto's surface is primarily composed of N_2 ice mixed in with CH_4 and CO at the mean surface temperature ~40 K. When averaged over its 250 year orbit, the poles receive more sunlight than the equator producing an atmosphere and resulting in transport to the equatorial regions [2]. Our understanding is largely based on rare occultation observations 1988 (pre-perihelion), 2002 and 2006 (post-perihelion) [3; 4]. A surface pressure between 6.5-24 μbars and a peak atmospheric temperature of ~100K at a radial distance ~1250km was inferred [3]. However, because of its low gravitational energy, 0.008eV/amu, escape to space results in significant mass loss on each orbit. Therefore, many studies of Pluto's evolution have been aimed at understanding the atmospheric loss rate [5; 6; 7; 8]. Using results from the occultations and calculations of solar heating rates in continuum models of the upper atmosphere, a series of authors calculated escape rates from Pluto's atmosphere by considering a process referred to as slow hydrodynamic escape [7; 9; 10]. Here we describe thermally-driven atmospheric escape from Pluto using a hybrid continuum/kinetic model in order to re-calculate the escape rate.

Escape from an atmosphere occurs most efficiently in the exosphere where molecular collisions are rare. The lower boundary to this region is called the exobase, r_x. The Jeans parameter, λ, is often used to evaluate the atmospheric escape rate: λ = gravitational energy/thermal energy = $(GM_p m/r)/(kT)$, where G is the gravitational constant, M_p planet mass, m the molecular mass, k the Boltzmann constant, r the radial position and T the temperature at r. At large $\lambda(r_x)$, escape occurs on a molecule by molecule basis, similar to evaporation, and referred to as Jeans escape. At small $\lambda(r_x)$ escape occurs as bulk outflow, referred to as hydrodynamic escape. The slow hydrodynamic escape model (SHE), considered intermediate to these, has been suggested to be applicable to $\lambda(r_x) >\sim 10$ [11]. Many atmospheres have intermediate to large λ: i.e., $\lambda(r_x)$ ~10, ~50, ~200 ~350 for Pluto, Titan, Mars and Venus respectively. Recently, the SHE model was used to estimate escape rates from Pluto and Titan that are orders of magnitude larger than the Jeans rates. Tucker and Johnson (2009) [12] showed that estimate for Titan's atmosphere was incorrect. In addition, when the temperature in Titan's atmosphere was artificially increased so that $\lambda(r_x)$ ~11, similar to that at Pluto, the escape rate

27th International Symposium on Rarefied Gas Dynamics, 2010
AIP Conf. Proc. 1333, 1145-1150 (2011); doi: 10.1063/1.3562798
© 2011 American Institute of Physics 978-0-7354-0888-0/$30.00

obtained was only ~1.5 times the Jeans rate [12;13]. Recent extensive kinetic simulations of thermally-induced escape showed that the transition from hydrodynamic to a Jeans escape occurs at Jeans parameters much less than 10 and over a surprisingly narrow range of λ [14]. Therefore, we developed a fluid/kinetic approach to reevaluate escape from Pluto.

II. Jeans Escape and Slow Hydrodynamic Escape (SHE)

The density of planetary atmospheres decreases with increasing altitude with the degree of rarefaction expressed by a Knusden number, *Kn*. Here it is defined as the ratio of the mean free path of the molecules, l_c, to the scale over which the density changes by a factor of 1/e, the atmospheric scale height, $H = r/\lambda$: i.e.: $Kn = l_c/H$. At low altitudes, where $Kn << 0.1$, the atmosphere is dense and molecules collide frequently. With increasing altitude (larger *Kn*) collisions become increasingly infrequent with the exobase, r_x, defined at $Kn \sim 1$ [15]. At this altitude molecules can escape with a high probability if their velocity exceeds the escape speed and is directed outward. In the Jeans approximation it is assumed the speed distribution at the exobase is Maxwellian, so that the escape rate is $\varphi_J = \pi\, r_x^2\, n_x \langle v_x \rangle\, [1 + \lambda(r_x)]\, \exp[-\lambda(r_x)]$ for exobase density $n(r_x)$ and mean thermal speed $\langle v_x \rangle = (8kT_x/\pi m)^{1/2}$ [15].

In the SHE model the steady state Navier-Stokes equations, with the viscous term typically dropped, are applied to a one dimensional (1D) radial atmosphere. In this model the continuity equation leads to a constant net upward flow, φ, vs. radial distance from a lower boundary, r_o: $\varphi = 4\pi r^2\, n(r)u(r) = 4\pi r_o^2\, n_o u_o$ with $n(r)$ the number density, $u(r)$ the flow speed and their values at r_o are n_o and u_o. The radial momentum (pressure) equation for molecules of mass *m*, in which the viscous term is dropped, is:

$$dp/dr = n\left(d\Phi/dr - d(mu^2/2)/dr\right) \tag{1a}$$

with *p* the gas pressure (*nkT*) and Φ the gravitational energy ($GM_p m/r$). The corresponding energy equation is:

$$d\left\{\varphi\left(mu^2/2 + C_p T - \Phi\right) - 4\pi r^2 \kappa(T) dT/dr\right\}/dr = 4\pi r^2 Q(r) \tag{1b}$$

where C_p is the heat capacity, $\kappa(T)$ the thermal conductivity and *Q(r)* accounts for the solar heating and IR cooling rates. The SHE model is based on Parker (1968a, b) [16] for the supersonic flow of plasma from the Sun with n_o sufficiently large and $\lambda_o > \sim 10$. Watson et. al. (1981) [11] applied this model to early Earth and Venus atmospheres in which solar EUV heating drives escape. The flow is referred to as slow because the thermal energy (C_pT) dominates the bulk flow energy ($^1/_2 mv^2$) in the region of the atmosphere where the equations are applied. Above that region it is assumed that the thermal energy is efficiently transferred to flow energy. Therefore, although $\varphi \neq 0$, *u* is set equal to 0 in Eq. 1a and 1b below an upper boundary. Defining $\langle E\varphi \rangle_{ro}$ as the heat flow across r_o, and, as in [7], $\beta(r) = r_o^{-2}\, [\int_{ro} r^2\, Q(r)\, dr]$ with $\beta \rightarrow \beta_o$ as $r \rightarrow \infty$, the pressure and the heat flow are determined from:

$$p = p_o \exp\left[-\int_{r_o} \lambda(r) dr/r\right]\ ; \qquad \varphi\left(C_p T - \Phi\right) - 4\pi r^2 \kappa(T) dT/dr = \langle E\varphi \rangle_{r_o} + 4\pi r_o^2 \beta(r) \tag{2}$$

Specifying *n* and *T* at r_o, these equations are solved for assumed values of φ and $dT/dr|_r$. Solutions for *n* and *T* are regarded as valid out to an *r* where the bulk speed is a fraction of the local sound speed and then extrapolated requiring that *n* and $T \rightarrow 0$ as $r \rightarrow \infty$ [7]. The final φ and $dT/dr|_{ro}$ are those giving the best fit to the measured density profile.

Problems with a SHE model for molecular escape are discussed in [12; 13; 14]. Typically fluid models are applied when $Kn << 0.1$, but the SHE model at Pluto and Titan is continued into the region $Kn > 1$. Therefore, in the exosphere, where molecules can travel planetary scale distances without suffering a collision, these authors use the same expression for $\kappa(T)$. Even when significant escape does occur, the thermal energy conducted upward can be carried off in directions perpendicular to the flow instead of driving escape [13; 14]. This effect cannot be described using SHE, which forces the upwardly conducted energy to be converted to bulk flow. For instance, when all of the solar radiation is absorbed below r_o, $Q(r) = 0$ in Eq. 1b, an analytic approximation of the escape rate, $\varphi \sim [4\pi\, r_o\, \kappa(T_o)\, T_o/\Phi_o]$, was obtained within the SHE model [9]. That is, the energy conducted upward from r_o is proportional to φ. A comparison of escape rates at Pluto for $Q(r) = 0$ above r_o in Eq. 1b is instructive. For an N_2 atmosphere [$C_p = 7/2$ k, $n_o = 4\text{x}10^{12}$ cm^{-3}, $T_o = 88.2$ K, $r_o = 1450$ km, $\kappa(T) = (9.37$ erg cm^{-1} s^{-1} K$^{-2})T$] the analytic estimate is 4.8 x 10^{26} s^{-1}. The corresponding numerical result, without neglecting the C_pT term, is 5.4 x 10^{26} s^{-1} [7]. These are orders of magnitude larger than the Jeans rate of 6.9 x 10^{19} for $r_x = 2690$ km, $n(r_x) = 5.3\text{x}10^6$ cm^{-3}, $T(r_x) = 47.7$ K and $\lambda(r_x) = 23$ from [7].

III. Fluid/Kinetic Model

In the region of a planetary atmosphere where escape occurs most efficiently, $Kn \geq 0.1$, molecular transport transitions from being an organized flow to individual uncorrelated motions. To obtain the macroscopic properties of a rarefied gas flow, solutions to the Boltzmann transport equation or Monte Carlo simulations are required [17]. The direct simulation Monte Carlo (DSMC) method describes the flow by using a set of modeling molecules that can be used to represent both the local density and local speed distribution in the atmosphere. In a planetary atmosphere this is achieved by tracking the motions of these molecules in the gravitational field subject to mutual collisions. Collisions between molecules are calculated in discrete radial cells based on the local values of the relative speeds, cross section and density. Therefore, the DSMC model includes thermal conduction explicitly and is a direct method for describing the transition from collisional to free molecular flow. Such a model was applied to the tenuous region of Titan's atmosphere [12], resulting in large differences from the SHE model results.

The accuracy of energy transport in an atmosphere modeled using DSMC is related to how realistically molecular collisions can be described: e.g., by collision diameters or scattering potentials. For an appropriate set of collision parameters, the atmosphere evolves in a manner that depends upon n, T at the lower boundary of the DSMC domain, r_{od}, and on energy deposited by the incident solar radiation in the simulation domain. When molecules traverse the upper boundary of this domain, those with velocities greater than the escape velocity and directed outward are assumed to escape and the others are specularly reflected. The reflected molecules represent molecules with trajectories that would eventually return to the simulation domain. Since there is always some small probability of a molecular collision even as $r \rightarrow \infty$, we increase the upper boundary until the change in the escape rate is on average <5%.

Although a three dimensional (3D) simulations is used, the atmosphere is assumed to be spherically symmetric, so the resulting properties only have a radial dependence, consistent with the previous models for Pluto's atmosphere. The molecules are tracked in 3D but the velocities and positions are rotated to a common radial volume when the collision probabilities are evaluated. Certain restrictions ensure the validity of the results: *1)* particle motions over a time step independent of intermolecular collisions (time step << mean free time between collisions) and *2)* cell widths in the flow direction much smaller than l_c and H [17]. A kinetic model like the DSMC can, in principal, be applied to the entire atmosphere, but it is computationally more efficient to use a fluid model in the dense regions as discussed below.

In order to calculate accurate escape rates, we divide the atmosphere into two regions, a fluid and a DSMC region, and solve for the atmospheric structure produced by a fixed density and temperature at the lower boundary, r_o. The fluid model requires an assumed escape rate, φ, and the heat flow across the lower boundary, $\langle E\varphi \rangle_{ro}$. These are determined by escape at the upper boundary of the DSMC simulation and, when heat is deposited in the simulation region, by accounting for the heating rate, β_o. Therefore, we iteratively solve the fluid and DSMC models to obtain a consistent description. That is, for $Kn \leq 1$ we numerically solve Eqs. 2a and b to obtain $u(r)$, $n(r)$, and $T(r)$ for a set of escape parameters φ and $\langle E\varphi \rangle$ at r_o where $Kn(r_o) << 0.1$. The resulting densities and temperatures at a radius r_{od} where $Kn = 0.1$, which is about two scale heights below the nominal exobase, are then used as lower boundary conditions in the DSMC simulation up to an altitude many scale heights above the exobase, $Kn >> 1$. At the upper boundary we calculate the particle escape rate, φ, and the energy flow, $\langle E\varphi \rangle$. These parameters are then used at r_o to again solve the fluid equations, which in turn provide new conditions of density and temperature at $Kn(r_{od}) = 0.1$.

In the fluid model for the low Knudsen number regime, Eqs. 2a and 2b were solved simultaneously using 4th order Runge-Kutta method with adaptive radial step-size (Runge-Kutta-Fehlberg method), to ensure a relative tolerance of 10^{-8} for $n(r)$ and $T(r)$. The step-sizes were between 0.1 and 2 km with the finer resolution necessary to resolve the faster change in temperature near the lower boundary and the narrow heating peak. The heating/ cooling model in [7] was used for the net solar heating and radiative cooling. Since the heating and cooling rates depend on the temperature and density, iteration is required to find consistent temperature, density and heating profiles.

In the region where the DSMC model was applied, variable cell widths were used in the radial direction usually chosen to be 1/3 of the local mean free path and capped at 10% of the local density scale height for mean free paths larger than the local atmospheric e-folding. A time step of ~2 – 5 s conserved energy and was chosen such that the fastest molecules would suffer at most 1 collision. The number of representative molecules was chosen to ensure a sufficient number of molecules (>200) were in the upper most cell, typically we used several 10^3 -10^5 representative molecules to describe the region $Kn > 0.1$. The motions of the molecules in the DSMC simulations were integrated using a 4th order Runge-Kutta method. Collisions between atmospheric molecules were computed using both a hard

sphere model (HS) and a variable hard sphere model (VHS) [17]. To ensure consistency between the fluid and kinetic models, we also used the Larsen-Borgnakke (LB) approximation for internal energy and the VHS cross section is parameterized to the temperature dependent thermal conductivity typically used in the SHE model, e.g. $\kappa(T) = \kappa_o T^{\omega}$. Using $\omega = 1$ and $T(r_{od})$ we obtain a reference value for the HS cross section of $\sigma_{ref} = 8.8 \times 10^{-15}$ cm^2 based on data of Ref. [7]. For the VHS model the cross section depends on the relative collision speed c_r, $\sigma = \sigma_{ref}\,(c_o/c_r)$ where c_o is the average relative velocity at r_o assuming a Maxwellian speed distribution. For T vs. r in Pluto's upper atmosphere, the N_2 vibrational modes are neglected. Therefore, the LB method is used for the rotational modes with the internal energy for each molecule at the lower boundary of the DSMC regime, r_{od}, based on a Maxwell-Boltzmann energy distribution and neglecting IR cooling.

Comparisons of results for HS, HS-LB, VHS and VHS-LB are shown in Fig. 1a and b. Although the resulting density does *not* depend significantly on the collision model (e.g. for all results $r_x \sim 3700$ km), the model can impact the

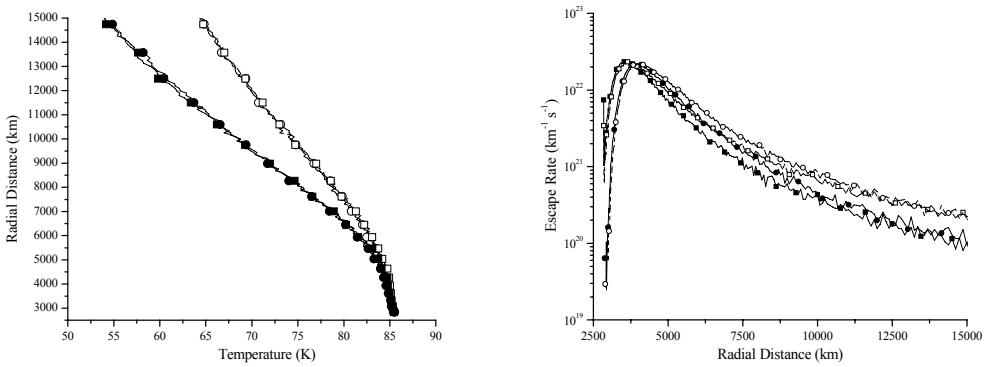

(a) **(b)**

FIGURE 1: (a) T(K) and (b) production of escaping molecules, $d\varphi/dr$ (km^{-1}s^{-1}) vs. r: HS (filled circles), VHS (filled squares), HS-LB (open circles), VHS-LB (open squares); $Q(r) = 0$ above lower boundary at $Kn(r_{od})=0.1$: exobase altitude is ~3700 km in all models.

temperature structure and the escape rate. For example, at the same lower boundary condition, $Kn(r_{od}) = 0.1$ and $\lambda(r_{od}) = 12$, the escape rates are 4.4, 5.1, 4.3 and 5.0 x10^{25} s^{-1} for the HS, HS-LB, VHS and VHS-LB models respectively. The peak in the escape rate production, Fig. 1b, occurs at the same altitude for the HS and VHS models with and without internal energy. But for the LB models above ~ 5000km, the internal and translation energies are not in equilibrium resulting in a larger escape rate and a higher temperature.

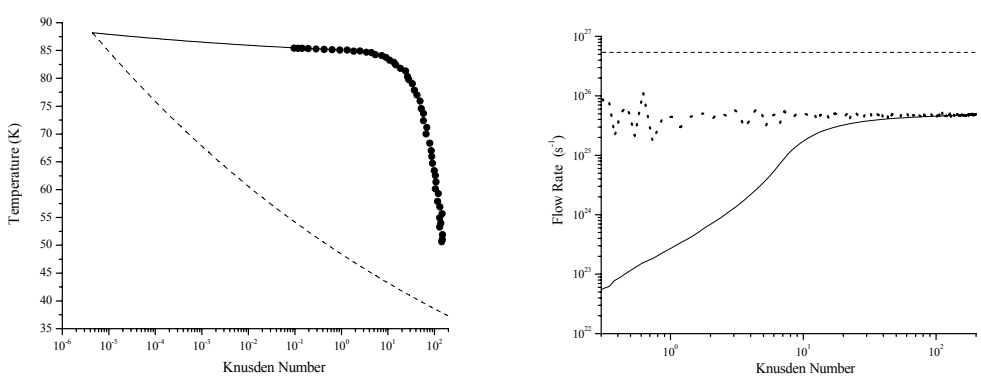

(a) **(b)**

FIGURE 2. (a)T(K) and (b) upward molecular flow in (s^{-1}) for $\beta_o = 0$ vs. position in the atmosphere given as $Kn(r)$; (a) dashed line: SHE model; solid line and filled circles: from fluid/DSMC; (b) net upward flow: dashed line, φ from SHE model; dotted line φ from fluid/DSMC: solid line, accumulated escape rate from DSMC.

IV. Results for Pluto's Atmosphere

Two cases were considered: with and without solar heating above our lower boundary r_o. The results in the previous section were calculated for $Q(r) = 0$ above r_o (i.e., β_o=0). Here we describe the more realistic case in which heat *is* deposited above r_o (β_o= 1.5x10^{-3} erg cm^{-2} s^{-1}) corresponding to solar minimum heating [7]. Solar medium and maximum conditions, for which the escape rates can be very large, will be described subsequently. In our iterative scheme we used the VHS-LB model in DSMC simulations. For lower boundary conditions, we use from ref. [7] $n(r_o)$ = 4x10^{12} cm^{-3} and $T(r_o)$ = 88.2 K at r_o = 1450 km. Since the fluid model also requires values of $\langle E\varphi \rangle$ and φ, for the β_o=0 case we began by assuming an isothermal, hydrostatic atmosphere $d(nkT_o)/dr = n\ [d\Phi/dr]$. Then a DSMC model starting at $Kn(r_{od})$ = 0.1 with HS cross sections was used to obtain the escape parameters. Those parameters are used as the starting values for the fluid/DSMC iterations in which we use the VHS-LB model in order to have $\kappa(T)$ and C_p consistent with the SHE model. For β_o=0 in the region where the fluid model and the DSMC model overlap, Kn ~ (0.1 – 1), the temperatures and densities are within < 2% in 3 iterations. Qualitatively consistent with the results in Tucker and Johnson 2009 [12], the escape rate obtained, 4.9 x10^{25}s^{-1}, is ~1.8 times the analytical Jeans escape rate, φ_J. Even though SHE model result gives $\lambda(r_x)$ ~23, which is

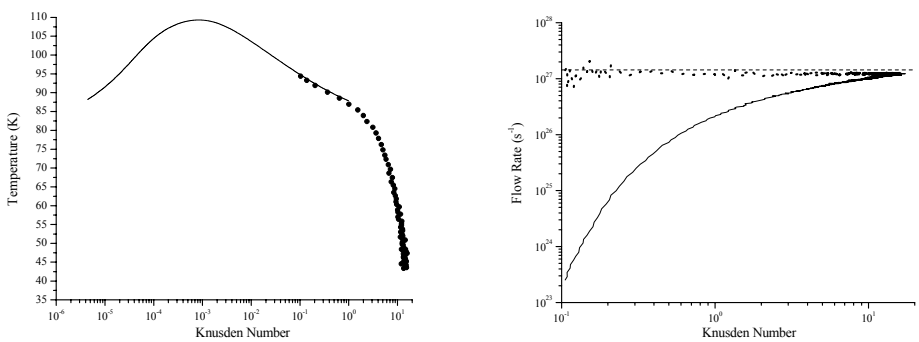

(a) **(b)**

FIGURE 3. (a) T(K) and (b) upward molecular flow in (s^{-1}) for β_o=1.5x10^{-3}erg cm^{-2} s^{-1} vs. position in the atmosphere given as $Kn(r)$: (a) solid line and filled circles: from fluid/DSMC simulation; (b) dashed line: φ from SHE model: dotted line: φ from fluid/DSMC; solid line: accumulated escape rate from DSMC part.

more than twice that from the fluid/DSMC model, [$\lambda(r_x)$ ~ 9], the SHE escape rate is an order of magnitude larger. The solutions for $n(r)$ and $T(r)$ are very different as well as seen in Fig. 2a. The change in temperature with increasing r falls off faster in the SHE solution. Furthermore, in Fig. 2b it is shown a significant drop in temperature does not occur until Kn ~ 10 where the net upward flux dominates the local density.

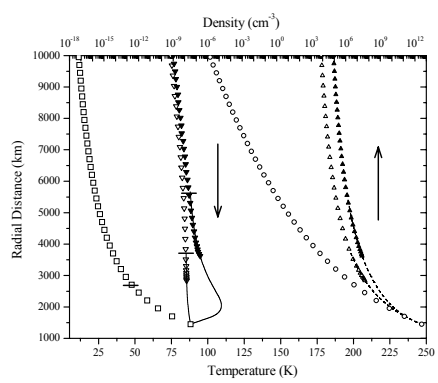

FIGURE 4. T(K) (lower axis), $n(r)$ (cm^{-3})(top axis); open squares: β_o = 0 from SHE; lines & open triangles: fluid/DSMC for β_o = 0; solid line & filled triangles: fluid/DSMC for β_o= 1.5x10^{-3}erg cm^{-2} s^{-1}: exobase marked by horizontal lines on $T(r)$ profiles.

Numerically solving the fluid equations for $\beta_o \neq 0$ is very sensitive to the choice of the input escape parameters, especially the escape rate, φ. Therefore, an initial solution was achieved by incrementally adding in a small fraction of the heating rate and solving the fluid equations assuming Jeans escape at the fluid upper boundary, Kn=1. We used $n(r_{od})$ and $T(r_{od})$ from that result evaluated at $Kn \sim 0.1$ as the starting point for the DSMC iteration and returned escape parameters to the fluid model as described above. The resulting escape rate was 1.2×10^{27} s^{-1} [$2.2 \cdot \varphi_J$ for $r_x \sim 5618$ km, $n_x \sim 1.\times 10^6$ cm^{-3}, $T_x \sim 87$ K and $\lambda(r_x) \sim 6$.] fortuitously similar to the SHE result, 1.5×10^{27} s^{-1}. However, for the SHE model, $r_x \sim 3530$ km, $n(r_x) \sim 3 \times 10^7$ cm^{-3}, $T(r_x) \sim 65$ K and $\lambda(r_x) \sim 13$ so the escape rate is $33 \cdot \varphi_J$, since the temperature near the exobase is low. The form of the integrated escape rate vs. r is similar to the $Q(r) = 0$ case; that is, there is a significant drop in temperature at $Kn \sim 10$ where the density is dominated by escape.

V. CONCLUSIONS

For a few decades, continuum models have been used to conclude that Pluto's atmosphere is lost by a process called slow hydrodynamic escape [7; 9; 10]**.** We tested this concept using a hybrid fluid/DSMC model and found that for the two cases considered, thermally-driven escape from Pluto occurs at a rate roughly similar to the Jeans rate. That is, for all of the heat deposited below the lower boundary, $\beta_o = 0$, and for solar minimum heating, $\beta_o = 1.5 \times 10^{-3}$ erg cm^{-2} s^{-1}, we obtain escape rates of $\sim 4.9 \times 10^{25}$ s^{-1}, which is ~1.8 times the Jeans rate, and 1.2×10^{27} s^{-1}, which is ~2.2 times the Jeans rate. As a further test of our hybrid model, we note that the results are consistent with recent results obtained using an intensive DSMC simulations of the entire atmosphere in the range Kn (0.0001 - 10) [14]. We also note that although the escape rate for the solar minimum case is fortuitously close to that from the SHE model, the temperature vs. altitude is very different. Therefore, in anticipation of the New Horizon encounter with Pluto in 2015, accurate simulations of the atmospheric structure and the escape rates will require the use of a hybrid model such as that described here.

Acknowledgements

Support from NASA's Planetary Atmosphere program (#NNX09AB68G) & NSF Astronomy program (#AST-0908378).

References

1 J. L. Elliot, et al., *Nature*, **424**, 165-167, pp. 165-167 (2003).
2 M. E. Brown, *Annual Reviews of Earth and Planetary Science* **30**, pp. 307-345 (2002).
3 J. L. Elliot, et. al., *The Astronomical Journal*, **134**, pp. 1-13 (2007).
4 E. F. Young, et al., *The Astronomical Journal*, **136**, pp. 1757-1769 (2008).
5 L. Trafton, *Icarus* **44**, pp. 53-61 (1980).
6 W. B. Hubbard, R. V. Yelle and J. I. Lunine, *Icarus*, **44**, pp. 53-61 (1990).
7 D. F. Strobel, *Icarus*, **55**, pp. 612-619 (2008a).
8 D. M. Hunten and A. J. Watson, *Icarus* **55**, pp. 665-667 (1982).
9 R. L. McNutt Jr., *Geophysical Research Letters*, **16**, pp.1225-1228 (1989).
10 V. A. Krasnopolsky, *Journal of Geophysical Research*, **104**, pp. 5955-5962 (1999).
11 A. J. Watson, T. M. Donahue and J. C. G. Walker, *Icarus* **48**, pp. 150-166 (1981).
12 O. J. Tucker and R. E. Johnson, *Planetary and Space Science*, **57,** pp. 1889-1894 (2009).
13 R. E. Johnson, *The Astrophysical Journal*, **716** pp. 1573-1578 (2010).
14 A. N. Volkov, O. J. Tucker, J. T. Erwin and R. E. Johnson, *Physics of Fluids*, submitted (2010).
15 R. E. Johnson, M. R. Combi, J. L. Fox, W.-H. Ip F. Leblanc, M. A. McGrath, V. I. Shematovich, D. F. Strobel and J. H. Waite Jr. **139**, pp. 355-397 *Space Science Reviews* (2008).
16 E. N. Parker, *The Astrophysical Journal*, **139**, pp. 664-676 (1958)
17 G. A. Bird, *Molecular Gas Dynamics and the Direct Simulation of Gas Flows, Oxford*: Oxford University Press, 1994.